Magnetic-field-induced enhancement of atomic stabilization in intense high-frequency laser fields

Aleksander Skjerlie Simonsen* and Morten Førre†
Department of Physics and Technology, University of Bergen, N-5007 Bergen, Norway
(Received 23 April 2015; published 9 July 2015)

The role of the magnetic-field component of the laser pulse on the phenomenon of atomic stabilization is investigated in an *ab initio* study. This is achieved by solving the time-dependent Schrödinger equation for the laser-atom interaction beyond the dipole approximation. The system under study is atomic hydrogen and the atom is assumed to be irradiated by an intense xuv laser light pulse of varying intensity and duration. We consider two different photon energies, $\hbar\omega = 54$ and 95 eV. The main finding is that there exists a range of laser pulse durations lasting for a few tens of field cycles where the atomic stabilization effect is enhanced due to the magnetic-field component. This is a rather surprising result that contradicts earlier statements made in the few-cycle pulse regime, where it has been shown that the magnetic field has a destructive effect in that the degree of stabilization is suppressed. It is further found that in the long-pulse limit the ionization probabilities obtained when illuminating the target with dipole and nondipole fields eventually coincide, meaning that the magnetic-field component of the laser field finally loses its significance in the context of atomic stabilization. It is also found that within the window of enhanced stabilization, the surplus population is distributed among excited bound states rather than in the initial ground state.

DOI: 10.1103/PhysRevA.92.013405 PACS number(s): 32.80.Rm, 42.50.Hz, 32.80.Fb

I. INTRODUCTION

Atomic stabilization is a physical phenomenon that was predicted theoretically more than 20 yr ago [1–13]. Independent studies of the ionization dynamics of hydrogen in intense, high-frequency laser fields produced an unexpected result: When raising the laser intensity up to a point where the applied forces are likely to dominate the Coulomb forces, it was found that the ionization process may eventually enter a regime of subsiding ionization probability or rate with increasing intensity or, alternatively, that the ionization yield levels out at a value lower than 1. This rather counterintuitive phenomenon was then dubbed atomic stabilization and was subject to much debate in the following years; see, e.g., [14–18], and references therein. The stabilization effect is expected to occur when the photon energy exceeds the binding energy of the given atomic system and for very high laser intensities, i.e., photon energies higher than 13.6 eV and intensities of more than 10^{16} W/cm^2 in the case of atomic hydrogen [8,19,20]. It has also been demonstrated that systems with more than one active electron are subject to stabilization, like, e.g., the helium atom [21,22]. The experimental technology enabling the production of xuv laser light bright enough to allow for the direct observation of atomic stabilization in ground state atomic systems has not yet come true. Instead, experimental attempts to measure the effect in excited atoms irradiated by optical laser fields have been pursued [23–28].

As atomic stabilization is expected to occur in the regime of high-intensity fields, it was pointed out early that the magnetic component of the laser field may no longer be neglected [29], i.e., that the electric dipole approximation becomes questionable. By performing quantum calculations beyond the dipole approximation (nondipole), some evidence of a possible breakdown of atomic stabilization of atoms interacting with intense high-frequency laser fields was predicted [30–32]. More recently, fully three-dimensional *ab initio* wave-packet calculations beyond the dipole approximation confirmed that the magnetic field may have a detrimental effect on the degree of stabilization, but that it nevertheless does not destroy the stabilizing effect altogether [20,33,34]. Furthermore, it has been shown that the excess continuum electrons, as released due to the nondipole field, are emitted with extremely low kinetic energy [34]. This emission of low-energy electrons is a characteristic of nondipole ionization dynamics in atoms [35] and molecules [36] in general. It is to be noted that, thus far, most *ab initio* studies have been pursued for relatively short laser pulses of durations limited up to a few tens of field cycles. The long-term evolution of atomic stabilization in hydrogen was explored in a recent work [37]. It was found that in the asymptotic limit of very long pulses the corresponding ionization rate does not anymore become influenced by the magnetic-field component, i.e., the dipole and nondipole results eventually coincide and the stabilizing effect persists.

The aim of the present work is to extend the investigation of the role of the magnetic-field component on atomic stabilization from the short-pulse regime into intermediate durations and ultimately, the long-pulse limit. We consider soft x rays, i.e., the two photon energies 54 and 95 eV, and the ionization dynamics of atomic hydrogen is studied beyond the dipole approximation. The main finding is that there is an intermediate-pulse regime where the stabilizing effect is enhanced due to the magnetic-field component of the laser field. This finding is rather surprising when seen in light of previous assumptions and in complete contradiction with the conclusions made in the series of studies performed in the short-pulse regime, where the magnetic field has been shown to be detrimental to stabilization [20,30–34]. Our conclusions are expected to be valid in the entire (nonrelativistic) high-frequency regime, provided that the photon energy exceeds the binding energy of the system at hand. Furthermore, in the limit of very long pulses the dipole and nondipole calculations are seen to produce very similar results, i.e., magnetic-field

*aleksander.simonsen@uib.no
†morten.forre@uib.no

effects are no longer of importance in the context of atomic stabilization dynamics, a result that is in agreement with recent findings [37].

We have further found that the magnetic-field-induced enhancement of stabilization seems to be accompanied by a significant increase of population in excited states as compared to its dipole approximation counterpart. It turns out that the electron is likely to become trapped in these states due to the influence of the magnetic field during the laser-atom interaction. We propose a population-trapping mechanism for explaining the increased stabilization and the corresponding higher survival probability. Performing calculations with various pulses, i.e., sine-square and Gaussian pulse profiles, different photon energies, and varying pulse durations and for a broad range of intensities, we have found that the population-trapping phenomenon and the corresponding enhanced stabilization effect are rather general phenomena, characteristic of strong-field ionization dynamics of atoms in high-frequency fields.

II. THEORY

The dipole approximation is one of the most common approximations in theoretical physics. Here the laser field is treated as a homogeneous time-dependent electric field; i.e., any spatial dependencies of the field as well as all effects due to the magnetic field are neglected. The dipole approximation is usually justified when the laser wavelength is much larger than the relevant atomic dimensions, provided that the intensity is not so high that magnetic-field effects [20,30–34] as well as relativistic effects [38–40] become important.

Assuming laser light propagating in the positive x direction and of linear polarization along the z axis and that the laser-atom interaction being nonrelativistic, the time-dependent Schrödinger equation (TDSE) in the velocity gauge for the dynamics of the hydrogen atom is given by

$$i\frac{\partial}{\partial t}\Psi(\boldsymbol{r},t) = \left\{\frac{1}{2}[\boldsymbol{p}+\boldsymbol{A}(\eta)]^2 - \frac{1}{r}\right\}\Psi(\boldsymbol{r},t). \tag{1}$$

Here $\boldsymbol{A}(\eta) = A(x,t)\hat{\mathbf{z}}$ is the time- and space-dependent vector potential defining the laser pulse, $\eta = \omega(t - x/c)$, ω is the central angular frequency of the field, and c is the speed of light. Atomic units where m_e, $\hbar$, e, and a_0 are scaled to unity have been introduced in Eq. (1). Solving Eq. (1) maintaining the full spatial dependence of the field is numerically involved. This is because the time and space coordinates are inextricably linked by the η parameter. To circumvent this problem, the vector potential can be written in terms of a power series. Expanding the vector potential to first order in powers of x/c yields

$$A(x,t) \simeq A(t) + \frac{x}{c}E(t), \tag{2}$$

$A(t)$ being the homogeneous z component of the vector potential and $E(t) = -\frac{d}{dt}A(t)$ the corresponding electric field. The TDSE takes the approximate form

$$i\frac{\partial}{\partial t}\Psi(\boldsymbol{r},t) \simeq \left[\frac{1}{2}p^2 - \frac{1}{r} + A(t)p_z + \frac{x}{c}A(t)E(t)\right]\Psi(\boldsymbol{r},t). \tag{3}$$

In deriving Eq. (3), and without loss of generality, the Coulomb gauge restriction $\boldsymbol{\nabla}\cdot\boldsymbol{A} = 0$ has been imposed, and the purely time-dependent and unimportant $\frac{1}{2}A^2(t)$ term has been removed through a phase (gauge) transformation [41]. Furthermore, all terms containing second- or higher-order powers of x/c have been neglected. Supplementary to this, the first-order spatial correction in the $\mathbf{A}\cdot\mathbf{p}$ operator is also omitted as it has proven to be unimportant to the nondipole ionization dynamics of hydrogen in xuv fields. The accuracy of the invoked approximations was assessed in a recent work [34], where it was shown that higher-order nondipole contributions in the expansion of the Hamiltonian but the one accounted for through the last term in Eq. (3) can safely be neglected. As such, the net nondipole effect is due to the (homogeneous) magnetic-field component of the laser pulse. The equation in the form (3) is the nondipole TDSE applied in the present work. The corresponding TDSE in the dipole approximation is retrieved by only keeping the homogeneous term from the expansion equation (2), i.e.,

$$i\frac{\partial}{\partial t}\Psi(\boldsymbol{r},t) \simeq \left[\frac{1}{2}p^2 - \frac{1}{r} + A(t)p_z\right]\Psi(\boldsymbol{r},t). \tag{4}$$

In solving the TDSE, the wave function is expanded on a basis composed of B-spline functions [42] for the radial coordinate and spherical harmonics for the angular part,

$$\Psi(\mathbf{r},t) = \sum_{klm} c_{klm}(t)\frac{B_k(r)}{r}Y_{lm}(\theta,\phi). \tag{5}$$

Note that with the inclusion of nondipole terms in the Hamiltonian the azimuthal symmetry of the problem is broken, i.e., all values of the magnetic quantum number m running from $-l$ to l need to be included in the expansion. The expansion (5) is truncated at some upper value of the orbital quantum number l, so that l runs from 0 to some maximum value $l_{\max}$. The B-spline functions $B_k(r)$ are distributed equidistantly in a box of length $R_{\max}$. B-spline functions are nonorthogonal but they have compact support; i.e., they are nonzero only on some finite interval [42]. This means that any operator may be represented as a sparse matrix, which is one of the main advantages of solving the TDSE directly in a B-spline-based basis. The result is that the memory consumption is significantly reduced as compared to a representation with global basis functions such as atomic eigenstates. The (stiff) system of ordinary differential equations in time that result from the B-spline expansion is then solved numerically by repeatedly applying the Cayley form propagator,

$$\left[\mathbf{S} + \frac{i\Delta t}{2}\mathbf{H}(t+\Delta t)\right]\mathbf{c}(t+\Delta t) = \left[\mathbf{S} - \frac{i\Delta t}{2}\mathbf{H}(t)\right]\mathbf{c}(t), \tag{6}$$

Δt being the propagator time step, and $\mathbf{S}$ and $\mathbf{H}$ the basis overlap and Hamiltonian matrices, respectively. Details about our computational scheme for solving the TDSE in order to obtain the wave function at the end of the laser pulse can be found in [34]. The probability of ionization and excitation of the system is then calculated by projecting the final wave function onto the complete set of bound and continuum energy eigenstates supported in the numerical box. For the problem at hand we obtain accurate numbers for the probabilities with $l_{\max} = 20$, $R_{\max} = 800$ a.u. and with 2400 B splines. It should

be noted, however, that while we obtain accurate values for the ionization probability with the present choice of $l_{\max}$, a much higher value of l is required if angular- or energy-resolved probability distributions are to be calculated [34].

III. RESULTS

Figure 1 shows the total ionization probability as a function of the electric-field strength for laser pulses of varying duration from 15 to 100 optical cycles (indicated with a number next to each curve). Results obtained in the nondipole [Eq. (3)] and dipole approximations [Eq. (4)] are shown in solid black and dashed red lines, respectively. The angular frequency of the laser field was set to $\omega = 3.5$ a.u., corresponding to the photon energy $\hbar\omega = 95$ eV. A sine-square temporal profile was imposed on the linearly polarized xuv laser field; i.e., the time variation of the corresponding vector potential followed

$$A(t) = \begin{cases} \frac{E_0}{\omega} \sin^2\left(\frac{\pi t}{T}\right) \sin(\omega t + \phi) & 0 \leqslant t \leqslant T, \\ 0 & \text{elsewhere.} \end{cases} \tag{7}$$

Here E_0 is the maximum electric-field amplitude, $\phi = 0$ is the carrier-envelope phase (CEP), and T defines the (total) pulse duration. In the present work, all pulses are relatively long in terms of optical cycles and as such the impact of the CEP on the results is negligible. From Fig. 1 it is seen that the dipole approximation breaks down at different field strengths depending on the duration of the pulse. For the 15-cycle pulse the dipole approximation is valid up to about $E_0 = 30$ a.u., whereas for the longest pulse considered (100 cycles), nondipole effects first become significant beyond $E_0 = 60$ a.u. We remark that relativistic effects might influence

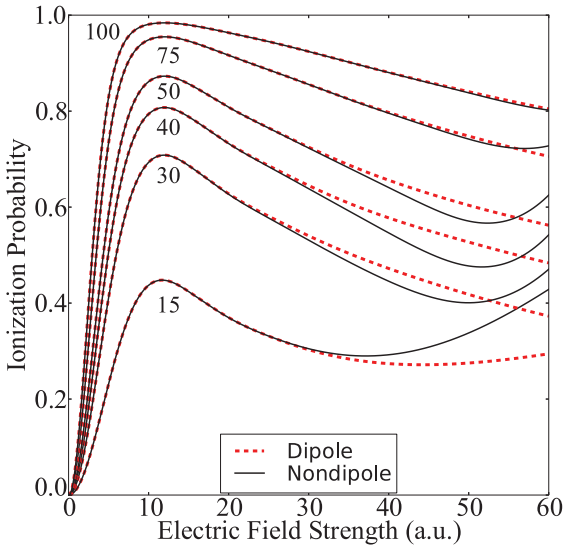

FIG. 1. (Color online) Total ionization probability vs electric-field strength for laser pulses of varying duration. The central angular frequency $\omega = 3.5$ a.u. and the temporal shape of the pulse is described by a sine-square carrier envelope. The pulse duration, given in number of field cycles, is indicated with a number next to each curve. Results obtained in the dipole approximation [Eq. (4)] and in the nondipole limit [Eq. (3)] are shown in dashed red and solid black lines, respectively.

the results at the very highest intensities considered in the figure ($E_0 \gtrsim 50$ a.u.), as the quiver velocity of a corresponding free (classical) electron in the laser field may exceed 10% of the speed of light. The decrease in the ionization probability with increasing laser intensity, which is the characteristic of the atomic stabilization phenomenon [14,15], is manifested at field strengths beyond $E_0 \simeq 12$ a.u.

Figure 1 shows that the importance of the magnetic-field component on the stabilization dynamics is highly sensitive to the pulse duration. For the shortest pulse, i.e., 15 cycles, the impact of nondipole effects is clearly destructive in that the degree of stabilization is suppressed when they are included, in particular for the highest laser intensities considered. So far, our findings are fully consistent with previously reported results in the short-pulse regime [20,30–34]. However, Fig. 1 also reveals a window of pulse durations where the total ionization probability is actually lowered when magnetic-field effects are taken into account. The effect is most distinct for the 30-, 40-, and 50-cycle pulse cases at intermediate laser intensities. This rather unusual dependence on the laser intensity stands in marked contrast to the corresponding behavior for shorter pulses, where the ionization probability is increased due to the magnetic field. As it turns out, for this magnetic-field-induced enhancement of atomic stabilization to occur, the electric field must be strong enough that the nondipole interaction, which is less important by a factor $1/c$ as compared to the regular dipole interaction, makes a significant contribution to the dynamics. However, it should still be weak enough and/or of long enough duration that the production of low-energy electrons due to nondipole shake-off processes [34] does not make a significant contribution to the ionization yield. In the case of the 40-cycle pulse, nondipole shake-off ionization becomes increasingly important above $E_0 \simeq 50$ a.u., with the result that the region of enhanced stabilization terminates at $E_0 > 56$ a.u. Nevertheless, for the longest pulses considered in Fig. 1 (75 and 100 cycles), the magnetic component eventually loses its significance. This means that in the limit of monochromatic fields any effect on the ionization yield due to the magnetic field vanishes and the dipole and nondipole results coincide, in agreement with recent findings [37]. As such, the phenomenon of magnetic-field-induced enhancement of atomic stabilization is expected to set in at intermediate pulse durations and for a finite interval of laser intensities.

In obtaining the results in Fig. 1, we have assumed that the approximation leading to the TDSE in Eq. (3) is valid, i.e., that the vector potential is expanded to first order in powers of x/c. We have explicitly checked that expanding the vector potential to second order in x/c yields essentially identical results for the ionization probability, even for the longest pulses considered. The validity of this approximation was also discussed in a recent work [34]. Furthermore, performing calculations in a significantly smaller numerical box, i.e., $R_{\max} = 40$ a.u. instead of $R_{\max} = 800$ a.u., and imposing an absorbing boundary to avoid unphysical reflections, the results for the ionization probability remain the same. This means that the relevant dipole and nondipole ionization dynamics takes place in the vicinity of the nucleus, and, as such, the approximate power series representation of the vector potential Eq. (2) seems appropriate.

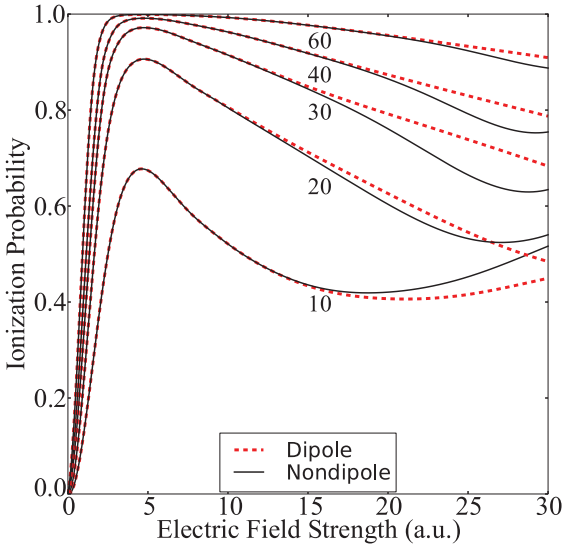

FIG. 2. (Color online) Same as Fig. 1, but with the driving field angular frequency $\omega = 2.0$ a.u.

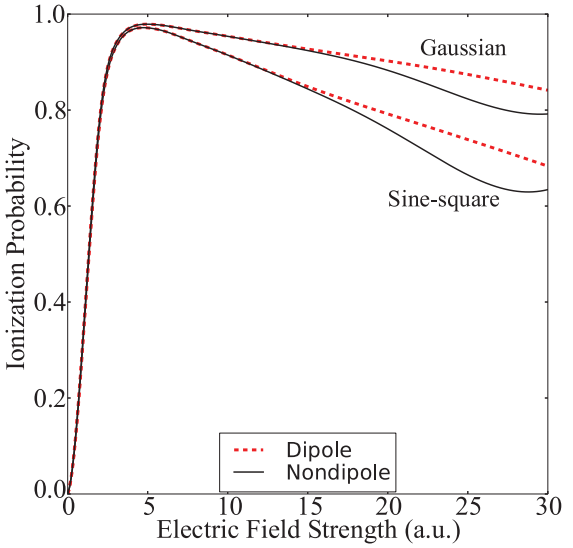

FIG. 3. (Color online) Total ionization probability vs electric-field strength for two laser pulses of different temporal profiles, i.e., sine-square and Gaussian, respectively. The total duration of the sine-square pulse corresponded to 30 optical cycles, and the mean photon energy $\hbar\omega = 2.0$ a.u. The Gaussian pulse is chosen so that both pulses have the same FWHM duration in the intensity domain. The nondipole results obtained with Eq. (3) and the dipole results [Eq. (4)] are drawn in solid black and dashed red lines, respectively.

As it turns out, the magnetic-field-induced magnification of the stabilization effect is a rather general phenomenon that occurs for other xuv photon energies as well. Figure 2 depicts the total ionization probability as a function of the electric-field strength obtained with a central angular frequency of $\omega = 2.0$ a.u. ($\hbar\omega = 54$ eV). The observed window of enhanced stabilization is somewhat different in this case, but the suppression of ionization due to beyond dipole dynamics is clearly expressed, most profoundly for the fields corresponding to 30 and 40 optical cycles. Naturally, the atomic stabilization effect, as well as the breakdown of the dipole approximation, set in at different electric-field amplitudes for this particular choice of frequency. Again, we recognize the short-pulse regime in which the stabilizing effect is suppressed (10-cycle field), the intermediate regime where it is enhanced (20–40 cycles), and finally the long-pulse limit (>60 cycles) where the dipole and nondipole results finally merge into each other.

Figure 3 shows a comparison of the dipole and nondipole ionization yields as obtained by laser pulses of different temporal profiles, i.e., a sine-square and a Gaussian profile. The reference pulse is the same as the one used in Fig. 2, i.e., $\omega = 2.0$ a.u. and a sine-square carrier envelope of duration 30 optical cycles. The other pulse comprises a field with the same angular frequency but with a Gaussian temporal profile instead,

$$A(t) = \frac{E_0}{\omega} \exp\left[-\frac{(t - T/2)^2}{2\sigma^2}\right] \sin\left[\omega(t - T/2) + \phi\right]. \quad (8)$$

The parameter σ here is the usual standard deviation of the Gaussian distribution and is set to $\sigma = 20.6$ a.u. With this choice, the two pulses have the same full width at half maximum (FWHM) duration in the intensity domain. Figure 3 reveals that, although the individual ionization probabilities obtained with the two different pulse shapes are not the same, presumably due to the different effective illumination at each spectral component, the overall picture is the same. The atomic stabilization effect is clearly expressed for both pulse shapes, but even more importantly, the window of enhanced stabilization due to nondipole dynamics also appears for the Gaussian pulse. As such, the results in Figs. 1–3 suggest that the magnetic-field-induced enhancement of atomic stabilization indeed is a rather general phenomenon that occurs for laser pulses of varying frequencies and shapes in the high-frequency regime. To this end, we have checked that an $\omega = 5$ a.u laser field yields similar conclusions.

The reason for the peculiar behavior at intermediate pulse durations is not yet clear, and in order to understand its origin

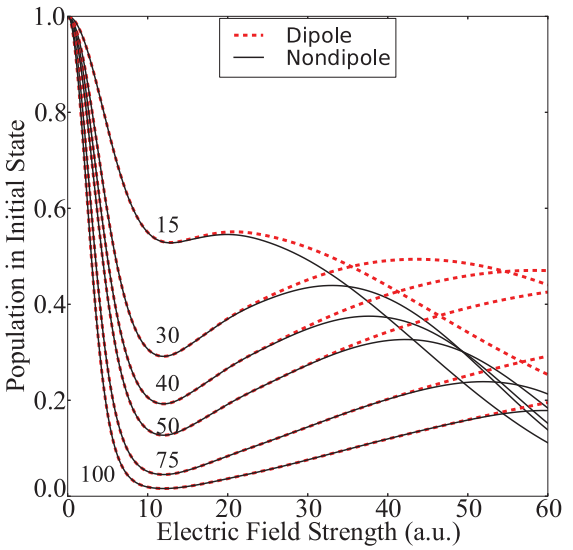

FIG. 4. (Color online) As Fig. 1, but the probability for the electron to remain in the initial ground state after the interaction with the xuv field.

we proceed to investigate the distribution of population among bound states. Figure 4 shows the remaining population in the initial (ground) state after the conclusion of the laser field for the same laser parameters considered in Fig. 1. We note that the population diminishes towards a local minimum close to the field strength $E_0 = 12$ a.u. for all pulse durations and that up to this point the dipole and nondipole results always coincide. As the field strength is increased beyond this point, entering the atomic stabilization regime, the dipole and nondipole initial-state probabilities eventually diverge from each other at different field strengths depending on the input pulse duration. More interestingly, the initial state population is consistently lower when the magnetic-field component is taken into account, which at first sight might seem odd considering the corresponding larger total survival probability (cf. Fig. 1). As a consequence, the remaining population must be accounted for among excited bound states, which prove to play an important role in the underlying nondipole induced dynamics.

Following these lines, the top panel in Fig. 5 depicts the corresponding population in all excited states as obtained in the nondipole limit for the same field parameters used in Figs. 1 and 4. The figure shows that these states constitute an important component of the final-state population for the higher field strengths and/or for the shorter pulse durations. In the most extreme cases considered here, almost half the population is found in excited states after the conclusion of the pulse. The increased population in these bound states in the limit of short and intense pulses can be understood from shake-up processes associated with the harsh ramp-on and ramp-off of the field. So far, these conclusions apply to both the dipole and the nondipole fields. When the pulse duration is increased, the nonadiabatic component of the field diminishes and shake-up processes play a less important role. Up to this point, the population in the excited states is not related to the impact of nondipole effects *per se*. However, a closer inspection shall reveal that the degree of excitation is very different for the dipole and nondipole fields, in particular within the window of intermediate pulse durations.

In the intermediate panel of Fig. 5 the difference in excitation probability between the nondipole and dipole results is plotted as a function of input laser intensity. For all pulse durations considered, this difference becomes a positive function of the electric-field strength; i.e., the population is always more likely to become trapped in excited states in the nondipole case. The most interesting aspect revealed in the figure is that the trapping effect is much more pronounced in the nondipole situation, in particular for the intermediate pulse durations. As such, the magnetic-field-induced enhancement of atomic stabilization goes hand in hand with the accumulation of population in excited states. For example, the pulse duration corresponding to 40 field cycles gave rise to the largest observed enhancement of stabilization at roughly $E_0 = 50$ a.u. (see Fig. 1), and this particular field also corresponded to the most extensive population growth in these states. Again, in the long-pulse regime the field becomes near monochromatic and the overall excitation probability diminishes both in the dipole and nondipole limits, respectively.

The two phenomena, magnetic-field-induced enhancement of atomic stabilization and the corresponding enhanced population of excited states seem to be intimately interconnected.

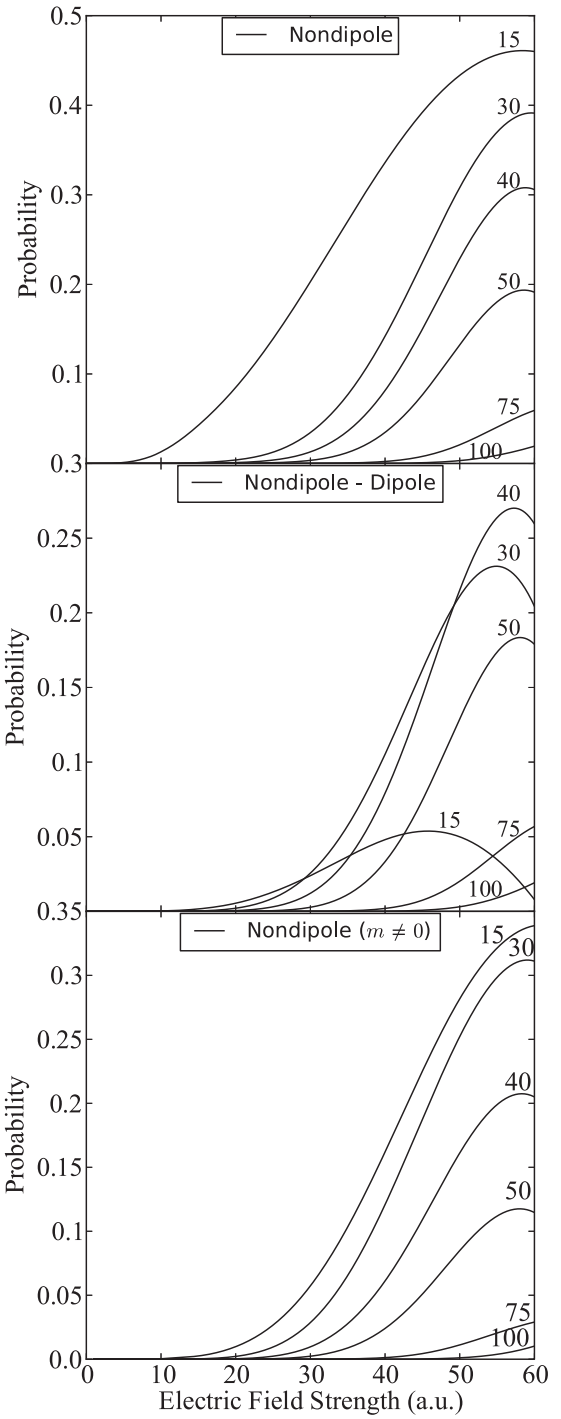

FIG. 5. (Top) As Fig. 1, but the total population in excited states after the interaction with the xuv field. Note that only the nondipole result obtained with Eq. (3) is shown. (Middle) The difference in excitation probability, $P_{\text{excited}}^{(\text{nondipole})} - P_{\text{excited}}^{(\text{dipole})}$, being taken between the nondipole and dipole results. (Bottom) The nondipole excitation probability shown exclusively for target states with $m \neq 0$.

Both phenomena may be explained in terms of a population-trapping mechanism: The nondipole part of the field allows for population of a wide range of states with magnetic quantum number $m \neq 0$ (dark states) during the laser-atom interaction. The importance of these states is illustrated in the bottom panel of Fig. 5, where the nondipole excitation probability is shown

for $m \neq 0$ bound states only. Comparing the results displayed in the top and bottom panels, we note that these dark states play a significant role for the bound population at the laser intensities high enough for observable magnetic-field effects. For all pulse durations considered here, $m \neq 0$ states comprise at least half the excitation probability and significantly more for the shorter and intermediate pulse durations. As such, the magnetic field allows for the population of a large set of excited bound states through Λ- or Raman-type two-photon transitions to states below the ionization threshold. In this process, one photon is absorbed from the field while the other is emitted. Once populated, the $m \neq 0$ states are metastable and do not couple to the ground state via the (dominating) electric dipole interaction. Furthermore, they are more resistant to ionization than the initial ground state, provided that the laser intensity is not too high. In effect, the states behave very much like dark states in the field, and the survival probability, hence degree of stabilization, grows larger because the bound population is trapped in these excited states. Such a trapping mechanism could explain why the magnetic-field component both enhances stabilization, and hence the survival probability, but simultaneously diminishes the ground-state population. Note that Λ- or Raman-type two-photon excitations ultimately become forbidden in the limit of monochromatic fields, simply due to the energy conservation rule, but they will be allowed in the intermediate-pulse regime where the enhanced stabilization effect is indeed observed.

IV. CONCLUSION AND SUMMARY

In summary, we have studied the ionization dynamics of atomic hydrogen illuminated by intense xuv laser light in the nondipole regime. To this end, we have solved the TDSE for the problem at hand from first principles in full dimensionality. The question of how and to what degree the magnetic-field component influences the phenomenon of atomic stabilization has been discussed for various input laser pulses. In previous studies it was established that the stabilizing effect tended to be diminished due to the magnetic field [20,30–34]. It is noteworthy that most of these studies were conducted for relatively short laser fields. We have extended the investigation in order to cover the whole spectrum from the short-pulse regime into the intermediate to long-pulse limit. The conclusion is that there are up to three different regimes of which the role of the magnetic field is rather different: First, in the short-pulse limit the stabilization is suppressed by the magnetic field, in agreement with earlier findings, and second, in the long-pulse limit the two interactions (dipole and nondipole) eventually yield very similar results. More interestingly, we have found that there exists a window of intermediate pulse durations where the survival probability is consistently increased in the nondipole limit, or, in other words, the stabilizing effect is enhanced. This behavior stands in complete opposition to the corresponding evolution at short fields. As it turns out, the magnetic-field-induced enhancement of atomic stabilization is a rather general phenomenon that applies to any high-frequency field of appropriate intensity. The enhanced stabilization effect is accompanied by a corresponding increase of population in excited states. We propose that these phenomena are related and that the enhanced survival probability is caused by a trapping mechanism which populates these states during the laser-atom interaction.

ACKNOWLEDGMENTS

This work was supported by the Bergen Research Foundation and the Norwegian Metacenter for Computational Science (Notur). Calculations were performed on the Cray XE6 (Hexagon) supercomputer installation at Parallab, University of Bergen (Norway).

[1] M. Gavrila and J. Z. Kamiński, Phys. Rev. Lett. **52**, 613 (1984).
[2] M. Pont, N. R. Walet, M. Gavrila, and C. W. McCurdy, Phys. Rev. Lett. **61**, 939 (1988).
[3] M. V. Fedorov and A. M. Movsesian, J. Phys. B **21**, L155 (1988).
[4] K. C. Kulander, K. J. Schafer, and J. L. Krause, Phys. Rev. Lett. **66**, 2601 (1991).
[5] K. Burnett, P. L. Knight, B. R. M. Piraux, and V. C. Reed, Phys. Rev. Lett. **66**, 301 (1991).
[6] M. Pont and M. Gavrila, Phys. Rev. Lett. **65**, 2362 (1990).
[7] Q. Su, J. H. Eberly, and J. Javanainen, Phys. Rev. Lett. **64**, 862 (1990).
[8] J. H. Eberly and K. C. Kulander, Science **262**, 1229 (1993).
[9] S. Geltman, J. Phys. B **27**, 257 (1994).
[10] S. Geltman, Chem. Phys. Lett. **237**, 286 (1995).
[11] R. Grobe and M. V. Fedorov, Phys. Rev. Lett. **68**, 2592 (1992).
[12] V. C. Reed, P. L. Knight, and K. Burnett, Phys. Rev. Lett. **67**, 1415 (1991).
[13] J. Parker and C. R. Stroud, Phys. Rev. A **41**, 1602 (1990).
[14] M. Gavrila, J. Phys. B **35**, R147 (2002).
[15] A. M. Popov, O. V. Tikhonova, and E. A. Volkova, J. Phys. B **36**, R125 (2003).
[16] K. Yamanouchi, S. L. Chin, P. Agostini, G. Ferrante, and M. Fedorov, in *Progress in Ultrafast Intense Laser Science I*, Springer Series in Chemical Physics Vol. 84 (Springer, Berlin, 2006), p. 1.
[17] M. Boca, H. G. Muller, and M. Gavrila, J. Phys. B **37**, 147 (2004).
[18] M. Gavrila, *Atoms in Intense Laser Fields* (Academic, New York, 1992).
[19] M. Dondera, H. G. Muller, and M. Gavrila, Phys. Rev. A **65**, 031405(R) (2002).
[20] M. Førre, S. Selstø, J. P. Hansen, and L. B. Madsen, Phys. Rev. Lett. **95**, 043601 (2005).
[21] T. Birkeland, R. Nepstad, and M. Førre, Phys. Rev. Lett. **104**, 163002 (2010).
[22] S. A. Sørngård, S. Askeland, R. Nepstad, and M. Førre, Phys. Rev. A **83**, 033414 (2011).
[23] R. R. Jones and P. H. Bucksbaum, Phys. Rev. Lett. **67**, 3215 (1991).
[24] M. P. de Boer, J. H. Hoogenraad, R. B. Vrijen, L. D. Noordam, and H. G. Muller, Phys. Rev. Lett. **71**, 3263 (1993).

[25] M. P. de Boer, J. H. Hoogenraad, R. B. Vrijen, R. C. Constantinescu, L. D. Noordam, and H. G. Muller, Phys. Rev. A **50**, 4085 (1994).
[26] N. J. van Druten, R. C. Constantinescu, J. M. Schins, H. Nieuwenhuize, and H. G. Muller, Phys. Rev. A **55**, 622 (1997).
[27] J. H. Hoogenraad, R. B. Vrijen, and L. D. Noordam, Phys. Rev. A **50**, 4133 (1994).
[28] L. D. Noordam, H. Stapelfeldt, D. I. Duncan, and T. F. Gallagher, Phys. Rev. Lett. **68**, 1496 (1992).
[29] T. Katsouleas and W. B. Mori, Phys. Rev. Lett. **70**, 1561 (1993).
[30] A. Bugacov, M. Pont, and R. Shakeshaft, Phys. Rev. A **48**, R4027 (1993).
[31] N. J. Kylstra, R. A. Worthington, A. Patel, P. L. Knight, J. R. Vázquez de Aldana, and L. Roso, Phys. Rev. Lett. **85**, 1835 (2000).
[32] J. R. Vázquez de Aldana, N. J. Kylstra, L. Roso, P. L. Knight, A. Patel, and R. A. Worthington, Phys. Rev. A **64**, 013411 (2001).
[33] K. J. Meharg, J. S. Parker, and K. T. Taylor, J. Phys. B **38**, 237 (2005).
[34] M. Førre and A. S. Simonsen, Phys. Rev. A **90**, 053411 (2014).
[35] M. Førre, J. P. Hansen, L. Kocbach, S. Selstø, and L. B. Madsen, Phys. Rev. Lett. **97**, 043601 (2006).
[36] M. Førre, S. Selstø, J. P. Hansen, T. K. Kjeldsen, and L. B. Madsen, Phys. Rev. A **76**, 033415 (2007).
[37] M. Y. Emelin and M. Y. Ryabikin, Phys. Rev. A **89**, 013418 (2014).
[38] Y. I. Salamin, S. X. Hu, K. Z. Hatsagortsyan, and C. H. Keitel, Phys. Rep. **427**, 41 (2006).
[39] S. Selstø, E. Lindroth, and J. Bengtsson, Phys. Rev. A **79**, 043418 (2009).
[40] A. Di Piazza, C. Müller, K. Z. Hatsagortsyan, and C. H. Keitel, Rev. Mod. Phys. **84**, 1177 (2012).
[41] A. V. Kim, M. Yu. Ryabikin, and A. M. Sergeev, Phys. Usp. **42**, 54 (1999).
[42] H. Bachau, E. Cormier, P. Decleva, J. E. Hansen, and F. Martín, Rep. Prog. Phys. **64**, 1815 (2001).